



# The $\delta^{15}\text{N}$ of chlorophyll to reconstruct the nitrate cycle in Adélie Land, East Antarctica, over the last 2000 years

Thibault SUTRE<sup>1,\*</sup>, Johan ETOURNEAU<sup>1,2</sup>, Xavier CROSTA<sup>1</sup>, Nanako O. OGAWA<sup>3</sup>, Robert McKay<sup>4</sup>, Hisami SUGA<sup>3</sup>, Naohiko OHKOUCHI<sup>3</sup>, Carlota ESCUTIA<sup>5</sup>

- 5 1 Université de Bordeaux, CNRS, Bordeaux INP, UMR 5805 EPOC, 33615 Pessac, France.  
2 EPHE/PSL Research University, 75014 Paris, France.  
3 Biogeochemistry Research Center, JAMSTEC, Yokosuka, 237-0061, Japan  
4 Antarctic Research Centre, Victoria University of Wellington, Wellington 6140, New Zealand  
5 Instituto Andaluz de Ciencias de la Tierra (IACT), CSIC, 28006 Madrid, Spain

10 *Correspondence to:* Thibault SUTRE (thibault.sutre@u-bordeaux.fr)

**Abstract.** The highly productive Antarctic coastal waters are a key component of the strong Southern Ocean biological pump, supported by high nutrient availability. However, modern observations of the nitrogen cycle and phytoplankton responses in these regions remain limited, particularly at multi-decadal to centennial timescales. The use of nitrogen stable isotopes ( $\delta^{15}\text{N}$ ) measured in chlorophyll *a* (Chl *a*) preserved in marine sediment offers a new opportunity to better understand the relationships  
15 between the past primary productivity, nitrate supply and environmental conditions. Because the  $\delta^{15}\text{N}_{\text{chl}}$  is directly derived from phytoplankton and is not affected by diagenetic alteration, it provides valuable insights into long-term changes in the nutrient cycle. Here we present the first antarctic  $\delta^{15}\text{N}_{\text{chl}}$  record from the well-dated U1357B IODP Site located offshore Adélie Land, East Antarctica, spanning the last two millennia. Our  $\delta^{15}\text{N}_{\text{chl}}$  record shows a strong variability with isotopic values oscillating between  $-6\text{‰}$  and  $-2\text{‰}$ . Comparison with other proxy reconstructions reveals periods of higher  $\delta^{15}\text{N}_{\text{chl}}$  at ~1850-  
20 1500 yrs BP and ~1100-500 yrs BP, corresponding to enhanced sea-ice cover and late seasonal melting. In contrast, lower  $\delta^{15}\text{N}_{\text{chl}}$  at 1500-1100 yrs BP and since 500 yrs BP coincide with less sea ice extent and earlier retreat. We interpret these variations in  $\delta^{15}\text{N}_{\text{chl}}$  as reflecting changes in nitrate supply from the subsurface nitrate-rich modified Circumpolar Deep Waters, driven by variations in sea-ice and atmospheric conditions over the last 2000 years.

## 1. Introduction

25 Understanding the marine biological carbon pump is essential for estimating the ocean's capacity to absorb atmospheric  $\text{CO}_2$  under global warming. The global ocean is estimated to absorb around 1.5-2.0 PgC per year (Takahashi *et al.*, 2009) through a combination of solubility-driven uptake and phytoplankton productivity (Gruber *et al.*, 2009). Approximately half of this oceanic  $\text{CO}_2$  uptake occurs in the rapidly changing Southern Ocean (Takahashi *et al.*, 2012; Hauck *et al.*, 2015). While phytoplankton productivity is generally limited in the high-nutrient, low-chlorophyll (HNLC) regions of the open Southern  
30 Ocean, it is particularly efficient in Antarctic coastal areas, where macro- and micronutrients (e.g. nitrate, silicate, and iron) are highly abundant (Deppeler and Davidson, 2017).



Coastal Antarctic phytoplankton communities are primarily composed of diatoms and soft-body tissue species developing mostly during the austral spring and summer (Sambrotto *et al.*, 2003; Beans *et al.*, 2008; Riaux-Gobin *et al.*, 2011). Sea-ice seasonality generally limits phytoplankton growth by reducing light penetration and by influencing vertical mixing, which controls the supply of nutrients from below the euphotic zone to the surface layer (Sambrotto *et al.*, 2003). In spring, sea-ice melt forms a stratified, nutrient-rich surface layer in which phytoplankton adapted to these conditions can develop significant blooms (Annett *et al.*, 2013), leading to a strong depletion of the surface nutrient stock (Sambrotto *et al.*, 2003) and aqueous CO<sub>2</sub> (DeJong and Dunbar, 2017). However, episodic wind-driven mixing and deepening of the surface mixed layer during the growing season enable access to the upper part of the nutrient-rich Circumpolar Deep Water (CDW) intruding onto the continental shelf (Lacarra *et al.*, 2011), thus sustaining high productivity until autumn (Annett *et al.*, 2010) and export of large amounts of organic carbon to the seafloor (Ratnarajah *et al.*, 2022; Stirnimann *et al.*, 2024).

Modern observations of nutrient cycling, especially nitrate (NO<sub>3</sub><sup>-</sup>), its controlling processes, and the responses of photosynthetic organisms remain limited in the sea-ice seasonal zone (DiFiore *et al.*, 2006; Henley *et al.*, 2018; Duprat *et al.*, 2020; Kim *et al.*, 2022). Together, they highlighted the spatio-temporal complexity of bioavailable nitrogen inputs into the surface layer, based on large-scale oceanography and regional mixing conditions, as well as interactions with local productivity. Additionally, oceanographic expeditions are generally limited to the austral spring-summer because the seasonality of the ice pack limits accessibility. Despite the increasing use of satellite observations, which now allow regular and global monitoring of the surface conditions throughout the year (Kahru *et al.*, 2010; Lacarra *et al.*, 2011; Carranza and Gille, 2015), processes occurring within the water column or below sea ice (e.g. nutrient and productivity) remain poorly constrained. The scarcity of observations spanning multi-decadal timescales limits our understanding of the long-term impacts of environmental variability on both the phytoplankton productivity and the nutrient cycles. Paleoenvironmental reconstructions are therefore critical for placing recent observations into a broader temporal context and unravelling the drivers of long-term changes in polar phytoplankton production.

Nitrogen stable isotope signals preserved in deep-sea sediments can provide insights into past nitrogen cycling beyond the instrumental period. During photosynthesis, phytoplankton preferentially assimilate the lighter N isotope (<sup>14</sup>N), leaving the residual seawater enriched in the heavier isotope (<sup>15</sup>N), which is ultimately transferred to the organic matter. As such, δ<sup>15</sup>N signals preserved in sediments reflect the degree of nitrate utilisation by the phytoplankton (Galbraith *et al.*, 2008), as a balance between supply and uptake, and their underlying processes (Altabet and Francois, 1994; Altabet, 2006). However, most studies exploring past changes in the Southern Ocean nitrogen cycle were conducted in the open ocean using nitrogen isotopic composition (δ<sup>15</sup>N) of bulk sediments (François *et al.*, 1997; Brzezinski *et al.*, 2002), diatom-bound organic matter (Robinson *et al.*, 2004; Studer *et al.*, 2015; Ai *et al.*, 2020; Fripiat *et al.*, 2026), or planktonic foraminifera (Marks *et al.*, 2023). Yet, studies have enabled the measurement of nitrogen isotopic composition of individual chlorophyll (δ<sup>15</sup>N<sub>chl</sub>) preserved in the sediment, providing a more direct record derived purely from phytoplankton (Chikaraishi *et al.*, 2008; Higgins *et al.*, 2011; Ohkouchi and Takano, 2014). Both the pigments' high resistance to fractionation processes, and their obligatory fast export and burying



65 to the sediment should benefit this study when trying to reconstruct past surface conditions. Such a proxy has indeed been successfully applied in several marine and lacustrine settings (Tyler *et al.*, 2010; Naeher *et al.*, 2016; Isaji *et al.*, 2022).

This study presents, for the first time, a  $\delta^{15}\text{N}$  signal extracted from chlorophyll *a* preserved in a sediment core from Adélie Land, East Antarctica (IODP Expedition 318, Site U1357B, Escutia *et al.*, 2011). As  $\delta^{15}\text{N}_{\text{chl}}$  had not yet been applied in Antarctic settings, we compare  $\delta^{15}\text{N}_{\text{chl}}$  with  $\delta^{15}\text{N}_{\text{bulk}}$  records from the same core to assess its potential for coastal Antarctic  
70 sediments. To further elucidate the factors controlling its variability, the record spanning the last 2000 years is examined through a multi-proxy approach to disentangle the dominant environmental drivers. We then discuss the potential implications of climate change for the coastal nitrogen cycle and the coastal Antarctic phytoplankton pump.

## 2. Study area

The Dumont D'Urville Trough (DDUT) off Adélie Land, East Antarctica, is characterised by several depressions shaped by  
75 past ice-stream activity and erosion processes (Leventer *et al.* 2006; McMullen *et al.*, 2006; Beaman *et al.*, 2011) (Fig. 1a). These depressions are separated by topographic highs and act as efficient sediment traps, facilitating the accumulation of material derived from surface productivity (Denis *et al.*, 2009; Johnson *et al.*, 2021). The DDUT is oriented southeast–northwest and extends from the French Dumont d'Urville Station to the continental slope. It is bordered by the Adélie Bank to the east and the Dibble Bank to the West, which limits the oceanic exchange along the continental shelf (Fig. 1a).

80 Hydrographically, the DDUT is influenced by multiple currents and water masses (Bindoff *et al.*, 2000; Williams *et al.*, 2010; Rintoul and Naveira Garabato, 2013). The main water masses relevant to phytoplankton productivity are the Antarctic Surface Water (AASW) and modified Circumpolar Deep Water (mCDW). Flowing westward, the AASW generally occupies the upper 100 m of the water column, where most phytoplankton develop, down to a local temperature minimum characterising the remnant Winter Water (WW) (Lacarra *et al.*, 2011). The AASW is characterised by low density ( $<28.03$ ) with rather low  
85 salinity ( $>34$  psu), and temperatures (from  $-1.8$  to  $-2.0$  °C) (Bindoff *et al.*, 2000) for the region, as well as a wide range of N nutrient concentration resulting from nitrate depletion due to successive phytoplankton blooms (e.g., nitrate concentration  $[\text{NO}_3^-]$  of  $\sim 16$ - $27$   $\mu\text{M}$ , Serebrennikova and Fanning, 2004). The CDW is advected by the Antarctic Circumpolar Current toward the continental shelf (Fig. 1a), where it penetrates through canyons at the shelf edge (Tamsitt *et al.*, 2017, 2021). CDW mixes with fresher shelf waters (Whitworth *et al.*, 1998), forming mCDW, which subsequently flows toward the inner shelf along  
90 through pathways (Lacarra *et al.*, 2011). The mCDW is a relatively warm ( $1.7 < \theta < 1.5$  °C), salty ( $< 34.7$  psu) (Bindoff *et al.*, 2000), and nutrient-rich water mass, with  $[\text{NO}_3^-]$  reaching  $\sim 35$ - $37$   $\mu\text{M}$  (Sigman *et al.*, 1999; DiFiore *et al.*, 2009). Because mCDW is lighter ( $28.0 < \gamma_n < 28.27$   $\text{kg m}^{-3}$ , Williams *et al.*, 2010a) than the underlying Antarctic Bottom Water (AABW) ( $\gamma > 28.27$   $\text{kg m}^{-3}$ , Bindoff *et al.*, 2000) and denser than AASW ( $\gamma < 28.03$   $\text{kg m}^{-3}$ , Bindoff *et al.*, 2000), it occupies an intermediate depth range between  $\sim 200$  and  $400$  m, where a temperature maximum is observed (DiFiore *et al.*, 2009).

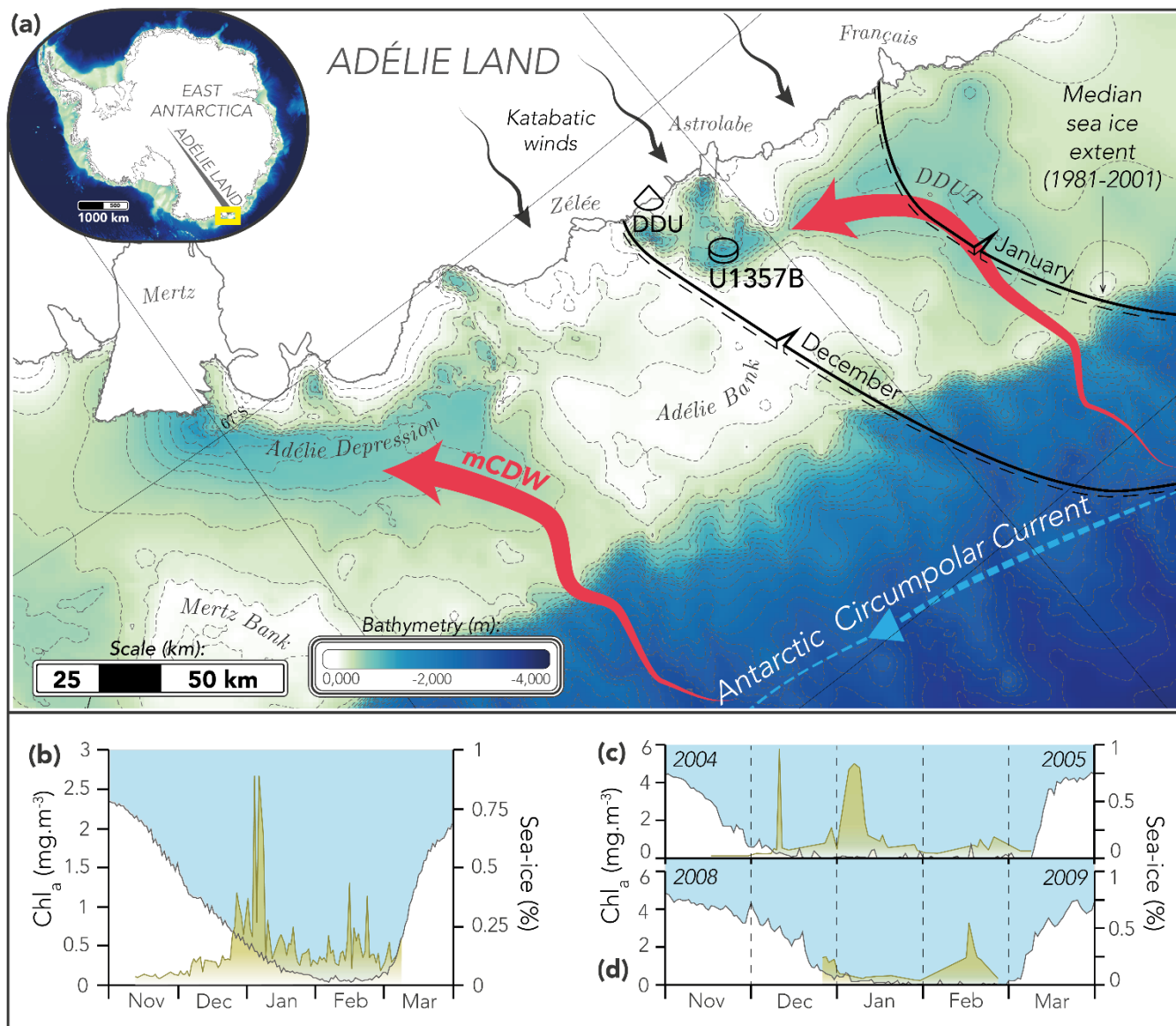
95 Over the DDUT, sea ice persists for 7 to 9 months per year (Fig. 1), typically from February-March to November-December (Fig. 1c & 1d) (Fetterer *et al.*, 2017). During winter, the mixed layer depth (MLD) deepens and homogenises the water column



through convection driven by sea-ice growth and brine rejection (Gordon and Huber, 1990; DiFiore *et al.*, 2009). Strong, episodic katabatic winds maintain the Dumont d'Urville polynya year-round (Parish and Wendler, 1991; Adolphs and Wendler, 1995; Wendler *et al.*, 1997), a major local source of sea-ice production that further enhances vertical mixing. In spring, sea-ice melt, combined with increasing daylight and atmospheric temperatures, leads to a shallow MLD and strong surface stratification.

The remnant Winter Water (or  $T_{\min}$  layer), whose deeper portion is isolated from the surface by spring stratification (Gordon and Huber, 1990; William *et al.*, 2010b), is acting as a source of intermediate  $[\text{NO}_3^-]$  between the surface layer and the richer mCDW (Sigman *et al.*, 1999). Because the WW partially inherited concentrations and isotopic signatures of the mCDW during winter high buoyancy-driven mixing, only the latter will be considered when discussing the nutrient exchanges with the subsurface. During summer, the MLD usually ranges between 50 and 100 m along the coast (Sigman *et al.*, 1999) and deepens episodically through the season owing to wind-driven mixing and progressive destratification (Williams *et al.*, 2010, Petty *et al.*, 2014). In this vein, the MLD observed near the Adelie Land coast can exceed 150 m during strong wind events (Vaillancourt *et al.*, 2003), enabling substantial vertical mixing and significant upward transport of nutrients from the mCDW into the subsurface (Carranza *et al.*, 2015). Consequently, the depth of the chlorophyll maximum, where nutrient concentration is elevated and light levels remain sufficient, follows that of the MLD (Vaillancourt *et al.* 2003).

In line with changes in sea-ice conditions, wind activity, and MLD, seasonal primary productivity in the Adélie Land typically can exhibit one to two chlorophyll production peaks associated with phytoplankton blooms. A main peak generally occurs in spring (late December–January), followed by a secondary one around February (Fig. 1b) (Massé *et al.*, 2011). However, the timing and intensity of these peaks vary from one year to another, with some years only showing enhanced production in spring or later in the summer (Fig. 1c & 1d) (Massé *et al.*, 2011). The exact drivers of this variability remain unclear, but likely include the timing of sea-ice retreat (Fig. 1c & 1d), surface water stratification, the direction and intensity of wind stress, and nutrient supply (Sambrotto *et al.*, 2003; Vaillancourt *et al.*, 2003; Beans *et al.*, 2008), all of which are modulated by climate variability (Denis *et al.*, 2006; Johnson *et al.*, 2021).



120 **Figure 1. a) Regional map of Adélie Land, East Antarctica. Red arrows: modified Circumpolar Deep Water (mCDW) trajectory**  
**through the depressions. Cylinder: IODP U1357 coring site. Cone: Dumont d'Urville (DDU) scientific station. Elevation from**  
**Matsuoka et al. (2021), bathymetry modified from Beaman et al. (2011), sea Ice extent from Fetterer et al. (2017). b) Average sea**  
**ice (1979-2014, in white) and surface chlorophyll (2002-2011, in green) concentrations during the austral summer season, over the**  
**DDUT. c) & d) Comparison of long and short ice-free seasons. Sea-ice concentrations from DiGirolamo et al. (2022) and surface**  
**chlorophyll concentrations from Massé et al. (2011).**

125



### 3. Materials & methods

#### 3.1 Sediment cores at the IODP 318 Site U1357B

The sediment cores at the IODP Site U1357B (Fig. 1) were collected during the IODP Wilkes Land Expedition 318 from the southern end of the DDUT, namely the Adélie Basin, (66°24.7990'S, 140°25.5705'E, 1028 m water depth, total length 170.7 m) in February 2010 (Escutia *et al.*, 2011) during the summer ice-free season (Fig. 1b). The collected sequences consist of continuously laminated diatom ooze with a high sedimentation rate (~1.5-2 cm yr<sup>-1</sup>) recording marine biogenic blooms (Johnson *et al.*, 2021). This study focuses on the upper 40 m of IODP core U1357B, which spans the last 2,000 years. The high-resolution age model was previously published in Johnson *et al.* (2021) based on eighty-seven <sup>14</sup>C dates, of which twenty were measured over the last 2,000 years.

#### 3.2 Pigments extraction and nitrogen isotope analysis

Chlorophyll *a* was extracted from freeze-dried sediment using 90% acetone by ultrasonication on ice for 5 min, followed by liquid-liquid extraction three times in *n*-hexane and Milli-Q water. The sediment was extracted up to three times and the combined *n*-hexane fraction was dried under Ar gas on a heater set to 30°C. The sample was then dissolved in 50 µL DMF (*N,N*-Dimethylformamide), before filtration through a 0.2 µm PTFE filter for HPLC analysis.

Purification of chlorophylls was performed with an analytical-scale column (ZORBAX XDB-C18, Agilent; 4.6 mm × 250 mm; 5-µm particle size) with a guard column. The pigments were eluted isocratically with 75% acetonitrile/pyridine (100:0.5, v/v) and 25% ethyl acetate/pyridine (100:0.5, v/v) for 5 min, followed by a linear gradient of ethyl acetate/pyridine to 50% over 50 min. The flow rate was set to 1 mL min<sup>-1</sup>, and the column temperature was set to 30°C. Peaks of chlorophyll *a* (Chl *a*) coeluting with divinylchlorophyll *a* (DVChl *a*) and chlorophyll *b* (Chl *b*) coeluting with divinylchlorophyll *b* (DVChl *b*) were separated and collected with baseline resolution.

The collected chlorophyll *a* was converted to pheophytin *a* by reaction with 2 M HCl. The converted pheophytins were completely dried, extracted with *n*-hexane and Milli-Q water three times, and the combined *n*-hexane fractions were dried under argon gas. The pheophytins *a* were then further purified by an analytical-scale column (Zorbax Eclipse PAH, Agilent; 4.6 mm × 250 mm; 5-µm particle size). The pigments were eluted isocratically with 80% acetonitrile/pyridine (100:0.5, v/v) and 20% ethyl acetate/pyridine (100:0.5, v/v) for 5 min, followed by a linear gradient of ethyl acetate/pyridine to 60% over 25 min, and then a linear gradient of ethyl acetate/pyridine to 100% over 10 min. The flow rate was set to 1 mL min<sup>-1</sup> and the column temperature to 15°C during the second purification process.

Stable isotopic compositions of both bulk sediment and the purified pigments were determined with a sensitivity-improved Flash EA1112 automatic elemental analyzer connected to a Thermo Finnigan Delta plus XP IRMS via a ConFlo III Interface (nano-EA/IRMS: Isaji *et al.*, 2020; Ogawa *et al.*, 2010). The purified pheophytins (80–350 ngN) were dissolved in chloroform, transferred quantitatively to a precleaned, smooth-wall, hard Sn capsules and dried completely before analysis. Nitrogen isotopic compositions are expressed in conventional δ notation relative to the atmospheric nitrogen (AIR). The analytical



160 precisions ( $1\sigma$ ) of the nano-EA/IRMS determined from replicate measurements of Ni-octaethylporphyrin as the laboratory standard were better than  $\pm 0.6\%$  for  $\delta^{15}\text{N}$ . The purities of the isolated compounds were confirmed by comparison with the estimated sample mass from the photoabsorbance of the HPLC and from the  $\text{N}_2$  peak of the nano-EA/IRMS.

### 3.3 Total organic carbon

165 The total organic carbon quantities (%TOC) were determined by the area of total ion peaks of the  $\text{CO}_2$  and  $\text{N}_2$  detected by the nano-EA/IRMS. Mass accumulation rates (MAR) for the total organic carbon were then calculated using the following formula:

$$\text{MAR} = \% \text{TOC} \times \text{LSR} \times \text{BD} \quad (1)$$

Where MAR = mass accumulation rate ( $\text{g.cm}^{-2}$  per year)

LSR = linear sedimentation rate ( $\text{cm per year}$ )

170 %TOC = the percent abundance (*as a decimal fraction*) of total organic carbon

BD = bulk density ( $\text{g.cm}^{-3}$ )

175 Linear sedimentation rates (LSR) were calculated using the Bayesian age-depth model for core U1357B (Ashley *et al.*, 2021). LSRs were calculated and binned into 10 cm intervals. No bulk density measurements were made for U1357B, therefore, bulk densities of discrete samples of the same ages from core U1357A were used. The U1357A age-depth model based on 36 bulk organic carbon dates, uses an identical Bayesian approach as U1357B (Johnson *et al.*, 2021). A linear fit model was constructed from the bulk densities data from U1357A, and this linear fit model was then interpolated onto the U1357B age scale to obtain an age versus density model for both holes. While this approach misses higher frequency variations in density, which are anticipated to be minor due to the consistent lithology, it does correct for downcore compaction.

180



## 4. Results

### 4.1 $\delta^{15}\text{N}$ and TOC records at site U1357B

The  $\delta^{15}\text{N}_{\text{chl}}$  at Site U1357B shows no trend over the past 2000 years, but exhibits a multi-decadal to multi-centennial variability between  $-6\text{‰}$  and  $-2\text{‰}$  (Fig. 2). The signal is rather stable before 1300 yrs BP, recording a mean of  $-3.3\text{‰}$ , before declining toward  $-5\text{‰}$  between 1250 and 1100 yrs BP. After a sharp increase of almost  $3\text{‰}$  around 1100 yrs BP, the isotopic signal remains high between 1100 and 600 yrs BP. Afterwards, the record depicts a decrease from  $-1.4\text{‰}$  at 617 yrs BP to  $-5.5\text{‰}$  at 272 yrs BP, then increases up to the maximum value of  $-0.8\text{‰}$  at 47 yrs BP.

In comparison, the  $\delta^{15}\text{N}_{\text{bulk}}$  signal at Site U1357B shows an almost continuous decreasing trend from  $\sim 5$  at 1800 yrs BP to  $\sim 2\text{‰}$  at the core top (Fig. 2). No centennial variability is superimposed on the decreasing trend.

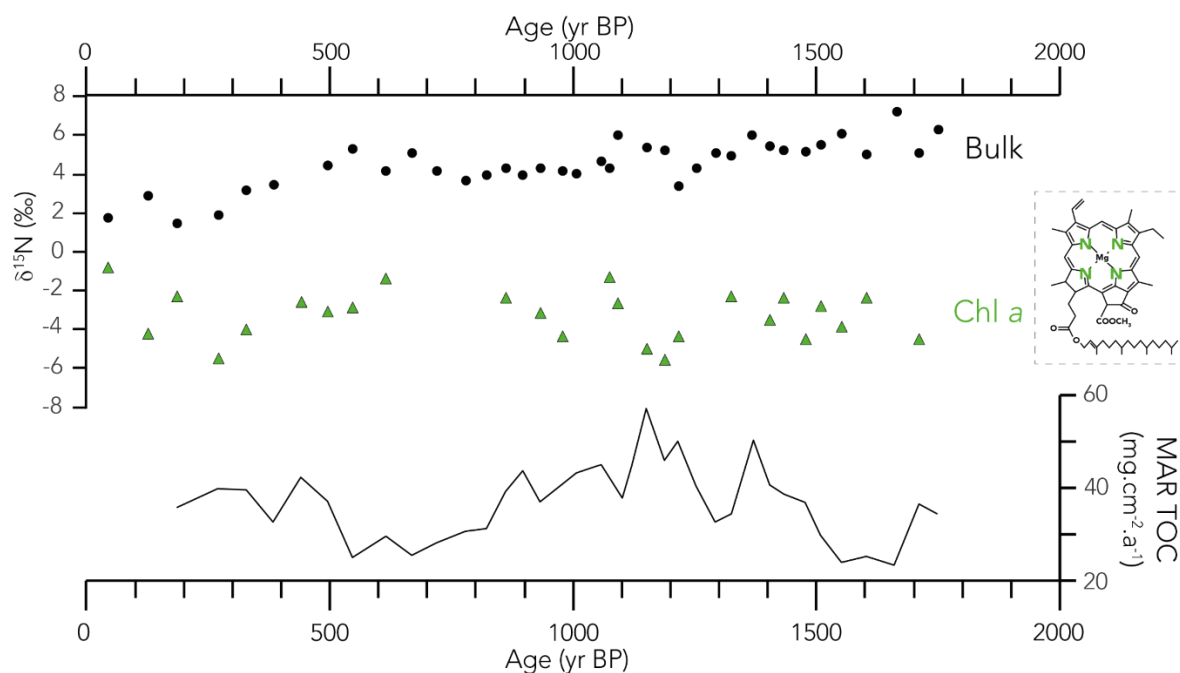


**Figure 2.**  $\delta^{15}\text{N}$  records of bulk nitrogen and chlorophyll *a*, and mass accumulation rates of total organic carbon measured from IODP core site U1357B over the last 2,000 years. Side frame displays the molecular structure of chlorophyll *a*.

195

The MAR TOC record also displays a strong variability over 2000 years (i.e. between  $\sim 23$  and  $\sim 57$  mg.cm<sup>-2</sup>.yr<sup>-1</sup>). Key multi-centennial trends are an increase from 23 mg.cm<sup>-2</sup>.yr<sup>-1</sup> at 1550 to 57 mg.cm<sup>-2</sup>.yr<sup>-1</sup> at 1150 yrs BP, interrupted by a local 35 mg.cm<sup>-2</sup>.yr<sup>-1</sup> minimum around 1300 yrs BP, and an extended decrease from the 1150 maximum to 25 mg.cm<sup>-2</sup>.yr<sup>-1</sup> at 550 yrs BP. After 500 yrs BP, the values stabilise at  $\sim 40$  mg.cm<sup>-2</sup>.yr<sup>-1</sup> up to 200 yrs BP.

200



## 5. Discussion

### 5.1 Rationale for the $\delta^{15}\text{N}_{\text{chl}}$ proxy in coastal Antarctic settings

205 In marine environments, the  $\delta^{15}\text{N}$  can be influenced by both N sources and sinks. Here, we exclude any significant impact of denitrification, the main N sink in the ocean, as a potential driver of  $\delta^{15}\text{N}$  variability. Denitrification predominantly occurs under weakly ventilated, low-oxygen and warm conditions typical of the mid- and low-latitude regions (Altabet, 2006), leading to the removal of bioavailable N and the enrichment of the residual nitrate pool (Fripiat *et al.*, 2023). Although denitrification has been previously reported in the western Antarctic Peninsula (Dutta *et al.*, 2023), its influence in the Adélie Basin is unlikely, given the persistently low  $\delta^{15}\text{N}$  values in both bulk and chlorophyll-derived records over the last 2,000 years.

210 Nitrogen ( $\text{N}_2$ )-fixation, the main source of fixed N to the ocean, is also unlikely to be a dominant control on  $\delta^{15}\text{N}$  variability in this region.  $\text{N}_2$ -fixation is primarily carried out by diazotrophic organisms that thrive in warm, nitrate-depleted, stratified waters, characteristic of some tropical and subtropical areas (Zehr & Capone, 2020). However, recent studies have reported evidence of  $\text{N}_2$ -fixation genes in the Adélie Basin (Shiozaki *et al.*, 2020) and off the northern Antarctic Peninsula (Pierrella *et al.*, 2021). The presence of these genes does not attest to an intense  $\text{N}_2$ -fixation activity. Though this assimilation process cannot be entirely ruled out and requires further investigation to properly quantify its contribution to the coastal Antarctica nitrogen cycle, these environments are generally considered unfavourable for sustaining high fixation rates (Raes *et al.*, 2020) because  $\text{N}_2$ -fixation is an energetically demanding process requiring high light availability (Kranz *et al.*, 2010).

215 Isotopic fractionation during nitrate uptake varies among phytoplankton groups and species (Needoba *et al.*, 2004), but this remains poorly constrained in coastal Antarctic environments. Although ammonium uptake occurs as an alternative nitrogen source (Goeyens *et al.*, 1995), previous studies indicated that nitrate is the primary N source supporting primary productivity off Adélie Land (DiFiore *et al.*, 2009), as confirmed by seasonal nitrate depletion coinciding with chlorophyll maxima (Sambrotto *et al.*, 2003). Sea ice and penguin colonies release nitrate, ammonium, and micronutrients such as iron, which may promote early-season phytoplankton blooms (Sedwick *et al.*, 1997; Otero *et al.*, 2018; Belyaev *et al.*, 2023). However, their contributions are likely negligible compared to inputs from the mCDW. The measured  $\delta^{15}\text{N}_{\text{NO}_3^-}$  (~20‰) and  $\delta^{15}\text{N}_{\text{TN}}$  (~10‰) in soils impacted by penguin guano around Antarctica (Wang *et al.*, 2020) are not consistent with the negative values found at IODP Site U1357.

220 Off Adélie Land, where nitrate is high,  $\delta^{15}\text{N}$  signals are expected to primarily reflect regional relative nitrate utilisation by phytoplankton, resulting from the balance between nitrate supply and biological uptake (Denis *et al.*, 2009; DiFiore *et al.*, 2009), with higher values indicating either increased uptake and/or reduced supply to surface waters. However, at site U1357B, 230 the reconstructed decrease in  $\delta^{15}\text{N}_{\text{bulk}}$  (from -2 to -6‰ over 2,000 years, Fig. 2), derived from a mixture of N-bearing compounds with variable and unquantified degrees of preservation, suggests instead a progressive downcore diagenetic enrichment in  $^{15}\text{N}$  due to preferential loss of  $^{14}\text{N}$  (Lourey *et al.*, 2003, Robinson *et al.*, 2012). Post-depositional alterations such as adsorption, remineralization, and terrestrial inputs may have further altered the original signal (Altabet *et al.*, 2006),



as previously hypothesised for the Southern Ocean (Altabet and Francois, 1994). This likely explains the lack of  
235 correspondence between the  $\delta^{15}\text{N}_{\text{bulk}}$  record and paleoenvironmental data derived from this site (Ashley *et al.*, 2020; Crosta *et al.*, 2021; Johnson *et al.*, 2021; Behrens *et al.*, 2022) or of larger geographical significance (Stenni *et al.*, 2017).

In contrast, the  $\delta^{15}\text{N}_{\text{chl}}$  reconstruction does not exhibit a long-term drift over the last 2,000 years (Fig. 2), attesting to its strong  
diagenetic resistance (Kashiyama *et al.*, 2008), as later specified. Yet, the unusually low  $\delta^{15}\text{N}_{\text{chl}}$  values (down to  $-6\text{‰}$ ),  
compared to  $\delta^{15}\text{N}_{\text{bulk}}$  values, as well as their pronounced multi-centennial millennial scale variability, raise the question of the  
240 processes and sources recorded in the  $\delta^{15}\text{N}_{\text{chl}}$ .

In the Adélie Basin, chlorophyll *a* is synthesised exclusively by phototrophic organisms, essentially diatoms with  
accompanying *Phaeocystis antarctica* (Wright and van den Eenden, 2000; Sambrotto *et al.*, 2003; Beans *et al.*, 2008; Stimimann  
*et al.*, 2024). Although chlorophyll *a* quickly degrades into derivative compounds (e.g., pheophytin *a* or pyropheophytin *a*)  
(Louda *et al.*, 2002; Chikaraishi *et al.*, 2007; Szymczak-Żyła *et al.*, 2008) under light and oxic conditions or during zooplankton  
245 grazing, diagenetic alteration of  $\delta^{15}\text{N}_{\text{chl}}$  remains minimal due to the robustness of its molecular nucleus (i.e., cyclic tetrapyrrole)  
containing four N atoms (Fig. 2) (Goericke *et al.*, 2000). As a result,  $\delta^{15}\text{N}$  values are largely preserved during deposition and  
early diagenesis (Ohkouchi *et al.*, 2005). Moreover, the labile nature of chlorophyll *a* implies that its preservation in sediments  
closely reflects surface water conditions at the time of production.

The very low  $\delta^{15}\text{N}_{\text{chl}}$  values are attributed to two reasons. First, nitrates are not the limiting factor for primary production in  
250 this region. Due to the preferential uptake of highly available  $^{14}\text{N}$ , partial nitrate assimilation leads to an apparent isotope  
fractionation toward lower values. Secondly, N isotopic fractionation happens during chlorophyll biosynthesis by eukaryotic  
algae, where chlorophyll *a* becomes depleted in  $^{15}\text{N}$  relative to bulk cellular N by an offset of  $4.8 \pm 1.4\text{‰}$  (Sachs *et al.*, 1999;  
Ohkouchi *et al.*, 2006). In addition,  $\delta^{15}\text{N}_{\text{chl}}$  depends on the bioavailable nitrogen pool in the Adélie Basin, which is largely  
dominated by seasonal inputs of nitrate-rich mCDW (DiFiore *et al.*, 2009). The initial  $\delta^{15}\text{N}$  of these nitrates ( $\delta^{15}\text{N}_{\text{nitrate}}$ ) has  
255 been measured in the Antarctic Zone and off Dumont d'Urville at  $4.8 \pm 0.2\text{‰}$  (Sigman *et al.*, 1999; DiFiore *et al.*, 2009).  
Accounting for isotopic fractionation during nitrate assimilation and chlorophyll biosynthesis explains the negative  $\delta^{15}\text{N}_{\text{chl}}$   
values recorded at Site U1357B, which is consistent with partial nitrate utilisation by phytoplankton.

In conclusion, despite uncertainties surrounding minor N sources, variations in  $\delta^{15}\text{N}_{\text{chl}}$  are expected to primarily reflect changes  
in relative nitrate utilisation in surface waters off Adélie Land over the last 2,000 years, resulting from the balance between  
260 the biological uptake by phytoplankton and physical supply of nitrate from the mCDW to surface waters.

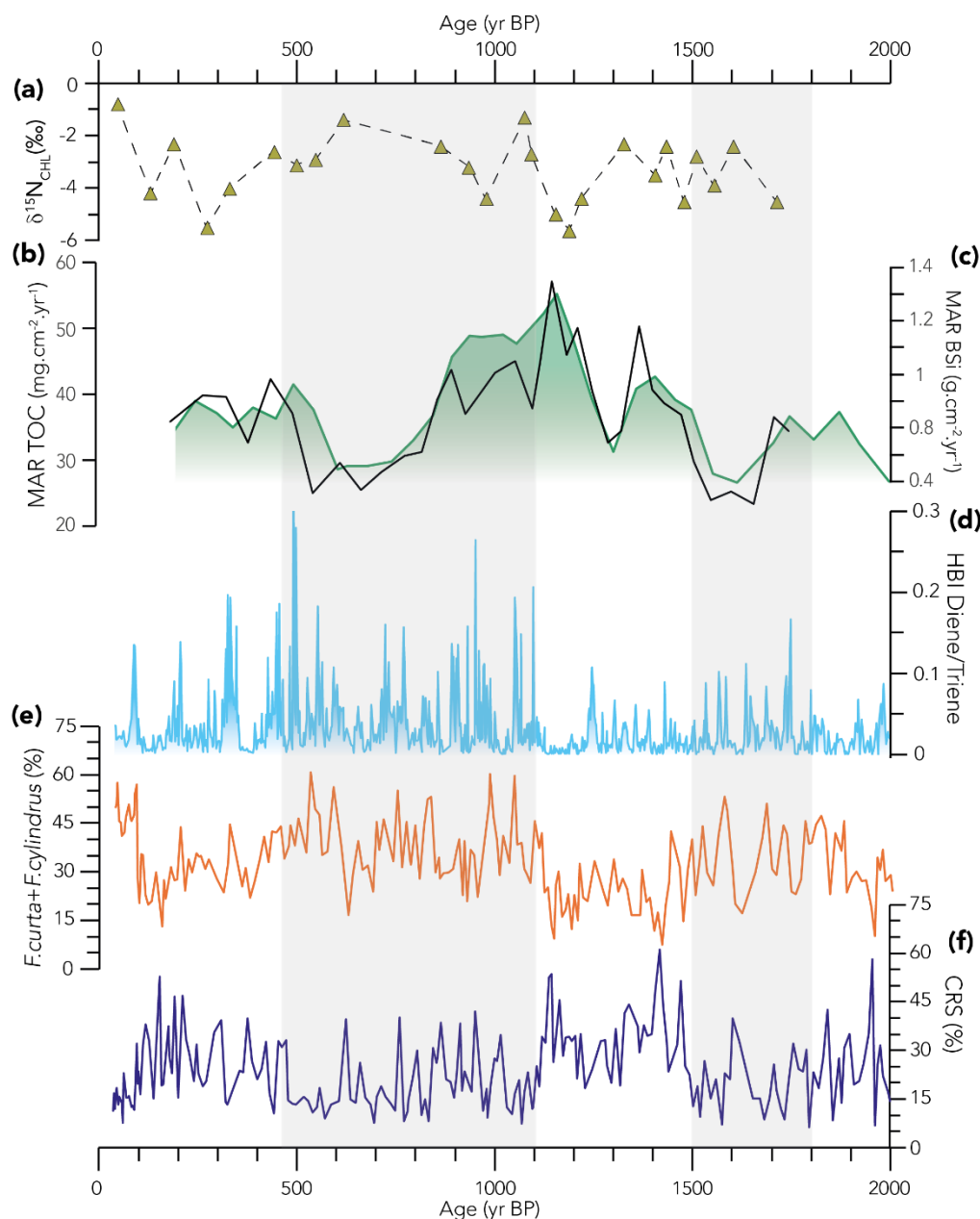


## 5.2 $\delta^{15}\text{N}_{\text{chl}}$ inferences on the nitrate cycle over the last 2,000 years

To discriminate the processes driving the variations in  $\delta^{15}\text{N}_{\text{chl}}$ , independent paleoenvironmental proxies from the U1357B core were selected. First, we document changes in total biological and in siliceous productivity using MAR TOC and MAR BSi, respectively, to assess the nitrate demand. The coherence between these two records (Fig. 3b & 3c) suggests that primary productivity in the Dumont d'Urville Trough (DDUT) was dominated by diatoms over the last 2000 years, as it is today (Beans *et al.*, 2008). Second, we document changes in sea ice using the HBI Diene/triene (Collins *et al.*, 2013; Belt *et al.*, 2016) and sea ice-associated diatoms (Campagne *et al.*, 2016). We also assess changes in water-column mixing using the relative abundances of *Chaetoceros* resting spores (Campagne *et al.*, 2016).

The MAR TOC and MAR BSi records show no similarity with the  $\delta^{15}\text{N}_{\text{chl}}$  during the last 2,000 yrs (Fig. 3a, 3b & 3c). For instance, between 1200 and 800 yrs BP, high and relatively stable BSi MAR values (e.g.,  $\sim 12 \text{ mg cm}^{-2} \text{ a}^{-1}$ ), indicative of efficient productivity and nitrate uptake by diatoms, coincide with a strong variability in  $\delta^{15}\text{N}_{\text{chl}}$  values (i.e. between  $\sim -6\%$  and  $\sim -2\%$ ). Subsequently, between 800 and 500 yrs BP, very low MAR BSi and MAR TOC values are congruent with elevated  $\delta^{15}\text{N}_{\text{chl}}$  values. As such, the MAR records show no temporal alignment with periods of elevated or reduced  $\delta^{15}\text{N}_{\text{chl}}$  described above. We cannot rule out that a part of the  $\delta^{15}\text{N}_{\text{chl}}$  variability can be due to nitrate uptake from non-siliceous phytoplankton groups, such as colonies of *Phaeocystis antarctica*. However, we believe that this impact is marginal as *P. antarctica* biomass is much less abundant than that of diatoms in nearby sites nowadays (Sambrotto *et al.*, 2003; Vaillancourt *et al.*, 2003). The discrepancy between the  $\delta^{15}\text{N}_{\text{chl}}$  record and both MAR signals (Fig. 3a, 3b & 3c) indicates that the degree of nitrate uptake by the regional productivity is unlikely to be the primary driver of  $\delta^{15}\text{N}_{\text{chl}}$  variability off Adélie Land. In this vein, a previous work in the region has suggested that  $\delta^{15}\text{N}_{\text{bulk}}$  variations from the neighbouring sediment core MD03-2601 were mostly driven by changes in nitrate supply rather than by changes in uptake (Denis *et al.*, 2009).

Reconstructing past nitrate supply can be partially achieved by characterising stratified conditions associated with sea-ice formation and melt, as well as wind-driven mixing that enabled access to nutrients from the mCDW. Mechanistically, sea ice exerts two synergistic effects on surface-water properties. First, its presence reduces wind stress at the surface ocean and limits the vertical mixing with underlying layers (Venables and Meredith, 2014). Second, enhanced meltwater input during sea-ice retreat freshens surface waters and increases stratification (Venables and Meredith, 2014). Together, these processes restrict the upward flux of nutrients from the subsurface waters and lead to a shallow MLD in spring. On the contrary, the summer MLD is primarily controlled by wind forcing and density gradients (De Boyer Montégut *et al.*, 2004), both being related to the absence of sea-ice cover. Consequently, variations in sea-ice extent, surface stratification, and wind-driven mixing provide a direct framework for interpreting changes in nitrate supply to surface waters. In the following section, we therefore use independent sedimentary proxies from Site U1357B to reconstruct past sea-ice conditions and water-column stratification, and to evaluate their respective roles in modulating nitrate availability and, ultimately,  $\delta^{15}\text{N}_{\text{chl}}$ .



295

300

**Figure 3. Intercomparison of relative nitrate utilisation, productivity, sea-ice and climate records from Site IODP U1357B. a)  $\delta^{15}\text{N}_{\text{chl}}$  (this study). b) Mass Accumulation Rates of total organic carbon (TOC, in black) (this study). c) Mass Accumulation Rates of biogenic silica material (BSi, in green) (Johnson et al., 2021). d) Di-unsaturated HBI (C25:2; Diene)/tri-unsaturated HBI isomer (C25:3; Triene) ratio (Ashley et al., 2021). e) Relative abundance of the combined *Fragilariopsis curta* and *Fragilariopsis cylindrus* group (Crosta et al., 2021). f) Relative abundance of *Chaetoceros Hyalochaete* resting spores (CRS) (this study; the protocol for the preparation of the slides, the counting rules, and the data acquisition follows the one described in Crosta et al., 2021). Grey areas highlight the periods of enhanced sea-ice cover and late seasonal melting.**



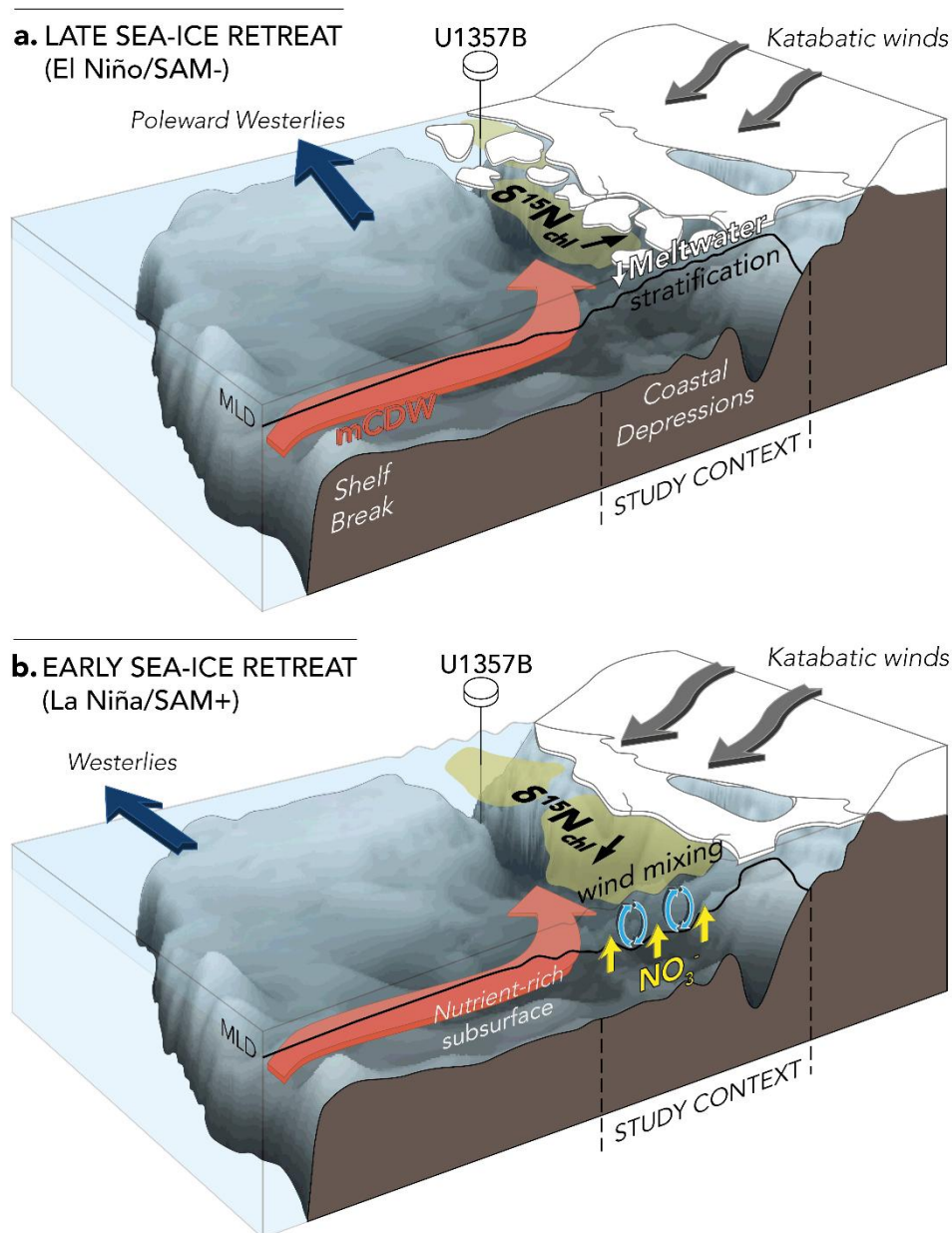
Sea-ice conditions are derived from the highly branched isoprenoids (HBIs), expressed as the ratio of diene to triene compounds (D/T), and the *Fragilariopsis curta* gp (combining *F. curta* and *F. cylindrus*). Higher values of D/T are linked to a greater presence of fast ice (Massé *et al.*, 2011, Belt *et al.*, 2016, Smik *et al.*, 2016) while higher percentages of the *F. curta* gp indicate a later melting of sea ice in spring (Campagne *et al.* 2016). In IODP Site U1357B, the D/T and *F. curta* gp records vary congruently and reveal two main intervals of enhanced sea-ice cover and late melting between ~1850-1500 yrs BP and ~1100-500 yrs BP, separated by periods of reduced sea ice (Fig. 3d & 3e) (Crosta *et al.*, 2021; Johnson *et al.*, 2021). Low relative abundances of *Chaetoceros Hyalochaete* resting spores (CRS) are synchronous with icier conditions (Fig. 3f). Comparison of diatom assemblages from an interface core collected in the inner DDUT and environmental parameters over the last 40 years attributed low CRS relative abundances to persistent stratification, reducing the nutrient availability, over the growing season (Campagne *et al.*, 2016). The combination of these records implies that increased sea-ice presence, during the two periods aforementioned, likely reduced wind stress, shoaled the MLD in spring while delaying its deepening in summer, and limited both the vertical water column mixing and nitrate supply to the surface (Fig. 3f & 4a). As a result, diminished nitrate availability led to higher  $\delta^{15}\text{N}_{\text{chl}}$  (Fig. 3a), despite a decrease in productivity observed during the last part of these periods (Fig. 3b & 3c). Conversely, an early retreat of sea ice, documented between 1500-1100 yrs BP and since 500 yrs BP (Fig. 3d & 3e), favoured wind-driven water-column mixing (Fig. 3f & 4b) and preconditioned a deeper summer MLD, which enhanced episodic nitrate supplies from the mCDW over the growing season. As a consequence, the nitrate pool increased, and the  $\delta^{15}\text{N}_{\text{chl}}$  declined. The regional productivity increased almost continuously during the 1500-1100 yrs BP period, peaking at ~1150 yrs BP (Fig. 3b & 3c) when  $\delta^{15}\text{N}_{\text{chl}}$  values reached their minimum (Fig. 3a). This may indicate that sufficient time existed between mixing events for water-column stabilisation and phytoplankton regrowth (Vaillancourt *et al.* 2003), but that the nutrient supply largely surpassed the phytoplankton demand as observed in low-latitude coastal upwelling systems (Robinson *et al.*, 2002; Rafter and Sigman, 2016).

As the siliceous and global productivities show little relationship with the relative nitrate utilisation and the environmental reconstructions, we believe that the primary control on the  $\delta^{15}\text{N}_{\text{chl}}$  signal is the renewal of the surface nutrient inventory through episodic summer nitrate supplies, particularly active when sea ice retreated early in the season. Any increase in the surface nitrate concentration would, however, be limited by the previous depletion of nitrates from earlier blooms and would be reflected in the  $\delta^{15}\text{N}_{\text{chl}}$  variations. The ability of the mixing conditions to overtake the productivity's influence over the  $\delta^{15}\text{N}_{\text{chl}}$  is therefore also attributed to the active renewal of mCDW-derived isotopically lighter nitrates in the surface for the later blooms to use.

Multi-decadal variability in sea-ice conditions off Adélie Land over the last 2000 years was largely driven by changes in large-scale atmospheric circulation patterns (Crosta *et al.*, 2021). During a persistent El Niño/SAM- combination, the SWW were located further to the south with a more southward direction, which enhanced sea-ice compaction at the coast (Fig. 4a). Congruently, lowered katabatic winds reduced vertical mixing and nutrient supplies during the growing season. Opposite atmospheric and sea-ice conditions were reconstructed during multi-decadal La Niña/SAM+ combinations (Fig. 4b). Consequently,  $\delta^{15}\text{N}_{\text{chl}}$  variability over the last 2,000 years is likely governed by the combined effects of changes in wind



regimes, sea-ice persistence, and access to mCDW nutrients, ultimately driven by the interplay between ENSO and SAM on multi-decadal timescales.



340 **Figure 4.** Schematic view of the environmental, sea-ice and mixing features during the early summer season (e.g., January) over the Dumont d’Urville Through, Terre Adélie, East Antarctica, and their effect on  $\delta^{15}\text{N}_{\text{chl}}$ . mCDW = modified Circumpolar Deep Water. MLD = Mixed Layer Depth. a) Mixing conditions in a situation of late sea-ice retreat (as observed during El Niño/SAM-combination). b) Mixing conditions in a situation of early sea-ice retreat (La Niña/SAM+).



## 6. Conclusions

345 This study represents the first use of the  $\delta^{15}\text{N}$  derived from chlorophyll *a*, recorded on a sediment core from the East Antarctic shelf. The robustness of the  $\delta^{15}\text{N}_{\text{chl}}$  allows to compensate for some defects in the more conventional  $\delta^{15}\text{N}_{\text{bulk}}$ . Here, without completely ruling out the influence of primary productivity on the signal, we show that nitrate inputs have changed significantly over the last two millennia in Adélie Land and are reflected in the  $\delta^{15}\text{N}_{\text{chl}}$ . Changes in supply were linked to the coupled action of winds and sea-ice conditions on the water column structure, with an early sea-ice melting leading to less stratified surface

350 water conditions, enhanced wind mixing, and recurrent nutrient recharge over the growing season, ultimately resulting in low  $\delta^{15}\text{N}_{\text{chl}}$  values. The decline in seasonal sea ice is unlikely to stop in the future, which may lead to a higher nutrient stock to fuel Wilkes Land's coastal Antarctic ecosystems, depending on the interactions between ENSO and SAM. Decreased stratification, increased nutrient availability, and warming waters during the growing season may shift communities from diatoms to less nutritious soft-tissue organisms. These changes could limit the export of organic carbon to the seafloor, with a

355 non-negligible impact on the uptake of  $\text{CO}_2$  by phytoplankton and profound changes to the surface water ecosystem. It is therefore necessary to accurately reconstruct the N cycle in coastal Antarctic regions presenting different atmospheric, oceanographic, and phytoplankton productivity conditions, to assess the Southern Ocean's role as a major storehouse of  $\text{CO}_2$  and distributor of nutrients to other oceans.

## Data availability

360 All new data presented in this paper can be found in the Supplementary materials.

## Author contributions

TS, JE, and XC wrote the manuscript. The samples were retrieved during the IODP Expedition 318 led by CE with the involvement of JE and RM. NOg, HS and NOh developed the analytical protocols. JE, NOg and HS carried out the analyses at JAMSTEC, Yokosuka. RM provided the total organic carbon record. XC provided the diatom abundance records. All

365 authors contributed to the interpretations of data and finalization of the manuscript.

## Acknowledgments

Samples and data were provided by the International Ocean Discovery Program (IODP). We thank IODP-France, which supported the participation of JE to the sampling party. We thank members of the ESF PolarClimate HOLOCLIP and IODP 318 Expedition for discussions. We sincerely thank the Dr. Chisato YOSHIKAWA and Yuta ISAJI, as well as the Dr. Mar

370 BENAVIDES, Jill SUTTON, Jean-Philippe FAIVRE and Nicolas SAVOYE for their assistance with scientific discussions and for mentoring the first author's current PhD.



### Competing interests

375 The authors declare no competing interests.

### Financial Support

This research has been supported by the French EMERGENCE – UPMC program 2012, Japanese Society for the Promotion of Science (JSPS/FF1/385 no. PE12506), the ERC StG ICEPROXY project (203441), the ANR CLIMICE project, the FP7 Past4Future project (243908), the BNP Paribas Foundation PHYTOPLANKTON, the New-Zealand MBIE ASIS, the bilateral  
380 FR-NZ PHC DDU MARICE, the IODP U.S. Science Support Program.

### References

- Adolphs, U., & Wendler, G. (1995). A pilot study on the interactions between katabatic winds and polynyas at the Adélie Coast, eastern Antarctica. *Antarctic Science*, 7(3), 307-314. [DOI: 10.1017/s0954102095000423](https://doi.org/10.1017/s0954102095000423)
- Ai, X.E., Studer, A.S., Sigman, D.M., Martínez-García, A., Fripiat, F., Thöle, L.M., Michel, E., Gottschalk, J., Arnold, L.,  
385 Moretti, S., Schmitt, M., Oleynik, S., Jaccard, S.L., Haug, G.H., 2020. Southern Ocean upwelling, Earth's obliquity, and glacial-interglacial atmospheric CO<sub>2</sub> change. *Science* 370, 1348–1352. <https://doi.org/10.1126/science.abd2115>
- Altabet, M.A., 2006. Isotopic Tracers of the Marine Nitrogen Cycle: Present and Past, in: Volkman, J.K. (Ed.), *Marine Organic Matter: Biomarkers, Isotopes and DNA*, The Handbook of Environmental Chemistry. Springer-Verlag, Berlin/Heidelberg, pp. 251–293. [https://doi.org/10.1007/698\\_2\\_008](https://doi.org/10.1007/698_2_008)
- 390 Altabet, M.A., Francois, R., 1994. Sedimentary nitrogen isotopic ratio as a recorder for surface ocean nitrate utilization. *Global Biogeochemical Cycles* 8, 103–116. <https://doi.org/10.1029/93GB03396>
- Annett, A.L., 2013. Phytoplankton ecology and biogeochemistry of the warming Antarctic sea-ice zone.
- Annett, A.L., Carson, D.S., Crosta, X., Clarke, A., Ganeshram, R.S., 2010. Seasonal progression of diatom assemblages in surface waters of Ryder Bay, Antarctica. *Polar Biol* 33, 13–29. <https://doi.org/10.1007/s00300-009-0681-7>
- 395 Ashley, K.E., McKay, R., Etourneau, J., Jimenez-Espejo, F.J., Condrón, A., Albot, A., Crosta, X., Riesselman, C., Seki, O., Massé, G., Golléde, N.R., Gasson, E., Lowry, D.P., Barrand, N.E., Johnson, K., Bertler, N., Escutia, C., Dunbar, R., Bendle, J.A., 2021. Mid-Holocene Antarctic sea-ice increase driven by marine ice sheet retreat. *Clim. Past* 17, 1–19. <https://doi.org/10.5194/cp-17-1-2021>



- Beaman, R.J., O'Brien, P.E., Post, A.L., De Santis, L., 2011. A new high-resolution bathymetry model for the Terre Adélie  
400 and George V continental margin, East Antarctica. *Antarctic science* 23, 95–103. <https://doi.org/10.1017/S095410201000074X>
- Beans, C., Hecq, J.H., Koubbi, P., Vallet, C., Wright, S., Goffart, A., 2008. A study of the diatom-dominated microplankton  
summer assemblages in coastal waters from Terre Adélie to the Mertz Glacier, East Antarctica (139°E–145°E). *Polar Biol* 31,  
1101–1117. <https://doi.org/10.1007/s00300-008-0452-x>
- Behrens, B.C., Yokoyama, Y., Miyairi, Y., Sproson, A.D., Yamane, M., Jimenez-Espejo, F.J., McKay, R.M., Johnson, K.M.,  
405 Escutia, C., Dunbar, R.B., 2022. Beryllium isotope variations recorded in the Adélie Basin, East Antarctica reflect Holocene  
changes in ice dynamics, productivity, and scavenging efficiency. *Quaternary Science Advances* 7, 100054.  
<https://doi.org/10.1016/j.qsa.2022.100054>
- Belt, S.T., Smik, L., Brown, T.A., Kim, J.-H., Rowland, S.J., Allen, C.S., Gal, J.-K., Shin, K.-H., Lee, J.I., Taylor, K.W.R.,  
2016. Source identification and distribution reveals the potential of the geochemical Antarctic sea ice proxy IPSO25. *Nat*  
410 *Commun* 7, 12655. <https://doi.org/10.1038/ncomms12655>
- Belyaev, O., Sparaventi, E., Navarro, G., Rodríguez-Romero, A., Tovar-Sánchez, A., 2023. The contribution of penguin guano  
to the Southern Ocean iron pool. *Nat Commun* 14, 1781. <https://doi.org/10.1038/s41467-023-37132-5>
- Bindoff, N.L., Rosenberg, M.A., Warner, M.J., 2000. On the circulation and water masses over the Antarctic continental slope  
and rise between 80 and 150°E. *Deep Sea Research Part II: Topical Studies in Oceanography* 47, 2299–2326.  
415 [https://doi.org/10.1016/S0967-0645\(00\)00038-2](https://doi.org/10.1016/S0967-0645(00)00038-2)
- Brzezinski, M.A., Pride, C.J., Franck, V.M., Sigman, D.M., Sarmiento, J.L., Matsumoto, K., Gruber, N., Rau, G.H., Coale,  
K.H., 2002. A switch from Si(OH)<sub>4</sub> to NO<sub>3</sub><sup>-</sup> depletion in the glacial Southern Ocean. *Geophysical Research Letters* 29.  
<https://doi.org/10.1029/2001GL014349>
- Campagne, P., Crosta, X., Schmidt, S., Noëlle Houssais, M., Ther, O., Massé, G., 2016. Sedimentary response to sea ice and  
420 atmospheric variability over the instrumental period off Adélie Land, East Antarctica. *Biogeosciences* 13, 4205–4218.  
<https://doi.org/10.5194/bg-13-4205-2016>
- Carranza, M.M., Gille, S.T., 2015. Southern Ocean wind-driven entrainment enhances satellite chlorophyll-a through the  
summer. *JGR Oceans* 120, 304–323. <https://doi.org/10.1002/2014JC010203>
- Chikaraishi, Y., Kashiyama, Y., Ogawa, N.O., Kitazato, H., Satoh, M., Nomoto, S., Ohkouchi, N., 2008. A compound-specific  
425 isotope method for measuring the stable nitrogen isotopic composition of tetrapyrroles. *Organic Geochemistry* 39, 510–520.  
<https://doi.org/10.1016/j.orggeochem.2007.08.010>
- Chikaraishi, Y., Matsumoto, K., Kitazato, H., Ohkouchi, N., 2007. Sources and transformation processes of pheopigments:  
Stable carbon and hydrogen isotopic evidence from Lake Haruna, Japan. *Organic Geochemistry* 38, 985–1001.  
<https://doi.org/10.1016/j.orggeochem.2007.01.005>
- 430 Collins, L.G., Allen, C.S., Pike, J., Hodgson, D.A., Weckström, K., Massé, G., 2013. Evaluating highly branched isoprenoid  
(HBI) biomarkers as a novel Antarctic sea-ice proxy in deep ocean glacial age sediments. *Quaternary Science Reviews* 79,  
87–98. <https://doi.org/10.1016/j.quascirev.2013.02.004>



- Crosta, X., Etourneau, J., Orme, L.C., Dalaiden, Q., Campagne, P., Swingedouw, D., Goosse, H., Massé, G., Miettinen, A., McKay, R.M., Dunbar, R.B., Escutia, C., Ikehara, M., 2021. Multi-decadal trends in Antarctic sea-ice extent driven by ENSO–  
435 SAM over the last 2,000 years. *Nat. Geosci.* 14, 156–160. <https://doi.org/10.1038/s41561-021-00697-1>
- De Boyer Montégut, C., Madec, G., Fischer, A.S., Lazar, A., Iudicone, D., 2004. Mixed layer depth over the global ocean: An examination of profile data and a profile-based climatology. *J. Geophys. Res.* 109, 2004JC002378. <https://doi.org/10.1029/2004JC002378>
- DeJong, H.B., Dunbar, R.B., 2017. Air-Sea CO<sub>2</sub> Exchange in the Ross Sea, Antarctica. *JGR Oceans* 122, 8167–8181.   
440 <https://doi.org/10.1002/2017JC012853>
- Denis, D., Crosta, X., Schmidt, S., Carson, D.S., Ganeshram, R.S., Renssen, H., Crespin, J., Ther, O., Billy, I., Giraudeau, J., 2009. Holocene productivity changes off Adélie Land (East Antarctica). *Paleoceanography* 24, 2008PA001689. <https://doi.org/10.1029/2008PA001689>
- Denis, D., Crosta, X., Zaragosi, S., Romero, O., Martin, B., Mas, V., 2006. Seasonal and subseasonal climate changes recorded   
445 in laminated diatom ooze sediments, Adélie Land, East Antarctica. *The Holocene* 16, 1137–1147. <https://doi.org/10.1177/0959683606069414>
- Deppeler, S.L., Davidson, A.T., 2017. Southern Ocean Phytoplankton in a Changing Climate. *Front. Mar. Sci.* 4. <https://doi.org/10.3389/fmars.2017.00040>
- DiGirolamo, N. E., C. L. Parkinson, D. J. Cavalieri, P. Gloersen, and H. J. Zwally, 2022: Sea ice concentrations from Nimbus-  
450 7 SMMR and DMSP SSM/I-SSMIS passive microwave data. NASA National Snow and Ice Data Center Distributed Active Archive Center, accessed 5 February 2024, <https://doi.org/10.5067/MPYG15WAA4WX>
- DiFiore, P.J., Sigman, D.M., Dunbar, R.B., 2009. Upper ocean nitrogen fluxes in the Polar Antarctic Zone: Constraints from the nitrogen and oxygen isotopes of nitrate. *Geochem Geophys Geosyst* 10, 2009GC002468. <https://doi.org/10.1029/2009GC002468>
- 455 DiFiore, P.J., Sigman, D.M., Trull, T.W., Lourey, M.J., Karsh, K., Cane, G., Ho, R., 2006. Nitrogen isotope constraints on subantarctic biogeochemistry. *J. Geophys. Res.* 111, 2005JC003216. <https://doi.org/10.1029/2005JC003216>
- Duprat, L., Corkill, M., Genovese, C., Townsend, A.T., Moreau, S., Meiners, K.M., Lannuzel, D., 2020. Nutrient Distribution in East Antarctic Summer Sea Ice: A Potential Iron Contribution From Glacial Basal Melt. *JGR Oceans* 125, e2020JC016130. <https://doi.org/10.1029/2020JC016130>
- 460 Dutta, A., Connors, E., Trinh, R., Erazo, N., Dasarathy, S., Ducklow, H.W., Steinberg, D.K., Schofield, O.M., Bowman, J.S., 2023. Depth drives the distribution of microbial ecological functions in the coastal western Antarctic Peninsula. *Front. Microbiol.* 14, 1168507. <https://doi.org/10.3389/fmicb.2023.1168507>
- Escutia, C., Brinkhuis, H., Klaus, A., n.d. IODP Expedition 318: From Greenhouse to Icehouse at the Wilkes Land Antarctic Margin.
- 465 Fetterer, F., K. Knowles, W. Meier, M. Savoie, and A. K. Windnagel. 2016, updated daily. Sea Ice Index, Version 2. [Indicate subset used]. Boulder, Colorado USA. NSIDC: National Snow and Ice Data Center. doi: <http://dx.doi.org/10.7265/N5736NV7>



- Fetterer, F., Knowles, K., Meier, W.N., Savoie, M., Windnagel, A.K., 2017. Updated Daily. Sea Ice Index, Version 3. <https://doi.org/10.7265/N5K072F8>
- 470 François, R., Altabet, M.A., Yu, E.-F., Sigman, D.M., Bacon, M.P., Frank, M., Bohrmann, G., Bareille, G., Labeyrie, L.D., 1997. Contribution of Southern Ocean surface-water stratification to low atmospheric CO<sub>2</sub> concentrations during the last glacial period. *Nature* 389, 929–935. <https://doi.org/10.1038/40073>
- Fripiat, F., Sigman, D.M., Ai, X.E., Dumoulin, C., Moretti, S., Studer, A.S., Diekmann, B., Esper, O., Frederichs, T., Lamy, F., Liu, L., Pattyn, F., Schmitt, M., Tiedemann, R., Haug, G.H., Martínez-García, A., 2026. Deglacial stratification of the polar Southern Ocean. *Proc. Natl. Acad. Sci. U.S.A.* 123, e2502076123. <https://doi.org/10.1073/pnas.2502076123>
- 475 Fripiat, F., Sigman, D.M., Martínez-García, A., Marconi, D., Ai, X.E., Auderset, A., Fawcett, S.E., Moretti, S., Studer, A.S., Haug, G.H., 2023. The Impact of Incomplete Nutrient Consumption in the Southern Ocean on Global Mean Ocean Nitrate  $\delta^{15}$  N. *Global Biogeochemical Cycles* 37, e2022GB007442. <https://doi.org/10.1029/2022GB007442>
- Galbraith, E.D., Sigman, D.M., Robinson, R.S., Pedersen, Thomas.F., 2008. Nitrogen in Past Marine Environments, in: *Nitrogen in the Marine Environment*. Elsevier, pp. 1497–1535. <https://doi.org/10.1016/B978-0-12-372522-6.00034-7>
- 480 Goericke, R., Strom, S.L., Bell, M.A., 2000. Distribution and sources of cyclic pheophorbides in the marine environment. *Limnology & Oceanography* 45, 200–211. <https://doi.org/10.4319/lo.2000.45.1.0200>
- Goeyens, L., Tréguer, P., Baumann, M.E.M., Baeyens, W., Dehairs, F., 1995. The leading role of ammonium in the nitrogen uptake regime of Southern Ocean marginal ice zones. *Journal of Marine Systems* 6, 345–361. [https://doi.org/10.1016/0924-7963\(94\)00033-8](https://doi.org/10.1016/0924-7963(94)00033-8)
- 485 Gordon, A.L., Huber, B.A., 1990. Southern ocean winter mixed layer. *J. Geophys. Res.* 95, 11655–11672. <https://doi.org/10.1029/JC095iC07p11655>
- Gruber, N., Gloor, M., Mikaloff Fletcher, S.E., Doney, S.C., Dutkiewicz, S., Follows, M.J., Gerber, M., Jacobson, A.R., Joos, F., Lindsay, K., Menemenlis, D., Mouchet, A., Müller, S.A., Sarmiento, J.L., Takahashi, T., 2009. Oceanic sources, sinks, and transport of atmospheric CO<sub>2</sub>. *Global Biogeochemical Cycles* 23, 2008GB003349. <https://doi.org/10.1029/2008GB003349>
- 490 Hauck, J., Völker, C., Wolf-Gladrow, D.A., Laufkötter, C., Vogt, M., Aumont, O., Bopp, L., Buitenhuis, E.T., Doney, S.C., Dunne, J., Gruber, N., Hashioka, T., John, J., Quéré, C.L., Lima, I.D., Nakano, H., Séférian, R., Totterdell, I., 2015. On the Southern Ocean CO<sub>2</sub> uptake and the role of the biological carbon pump in the 21st century. *Global Biogeochemical Cycles* 29, 1451–1470. <https://doi.org/10.1002/2015GB005140>
- Henley, S.F., Jones, E.M., Venables, H.J., Meredith, M.P., Firing, Y.L., Dittrich, R., Heiser, S., Stefels, J., Dougans, J., 2018. Macronutrient and carbon supply, uptake and cycling across the Antarctic Peninsula shelf during summer. *Phil. Trans. R. Soc. A.* 376, 20170168. <https://doi.org/10.1098/rsta.2017.0168>
- 495 Higgins, M.B., Wolfe-Simon, F., Robinson, R.S., Qin, Y., Saito, M.A., Pearson, A., 2011. Paleoenvironmental implications of taxonomic variation among  $\delta^{15}$ N values of chloropigments. *Geochimica et Cosmochimica Acta* 75, 7351–7363. <https://doi.org/10.1016/j.gca.2011.04.024>



- 500 Isaji, Y., Yoshikawa, C., Ogawa, N.O., Matsumoto, K., Makabe, A., Toyoda, S., Ishikawa, N.F., Ogawa, H., Saito, H., Honda, M.C., Ohkouchi, N., 2022. Nitrogen Sources for Phytoplankton in the Eastern Indian Ocean Determined From  $\delta^{15}\text{N}$  of Chlorophyll *a* and Divinylchlorophyll *a*. *Geochim Geophys Geosyst* 23, e2021GC010057. <https://doi.org/10.1029/2021GC010057>
- Johnson, K.M., McKay, R.M., Etourneau, J., Jiménez-Espejo, F.J., Albot, A., Riesselman, C.R., Bertler, N.A.N., Horgan, H.J.,
- 505 Crosta, X., Bendle, J., Ashley, K.E., Yamane, M., Yokoyama, Y., Pekar, S.F., Escutia, C., Dunbar, R.B., 2021. Sensitivity of Holocene East Antarctic productivity to subdecadal variability set by sea ice. *Nat. Geosci.* 14, 762–768. <https://doi.org/10.1038/s41561-021-00816-y>
- Kahru, M., Gille, S.T., Murtugudde, R., Strutton, P.G., Manzano-Sarabia, M., Wang, H., Mitchell, B.G., 2010. Global correlations between winds and ocean chlorophyll. *J. Geophys. Res.* 115, 2010JC006500.
- 510 <https://doi.org/10.1029/2010JC006500>
- Kashiyama, Y., Miyashita, H., Ohkubo, S., Ogawa, N.O., Chikaraishi, Y., Takano, Y., Suga, H., Toyofuku, T., Nomaki, H., Kitazato, H., Nagata, T., Ohkouchi, N., 2008. Evidence of Global Chlorophyll *d*. *Science* 321, 658–658. <https://doi.org/10.1126/science.1158761>
- Kim, B.K., Jeon, M., Park, S.-J., Kim, H.-C., Min, J.-O., Park, J., Ha, S.-Y., 2022. Variability in the Carbon and Nitrogen
- 515 Uptake Rates of Phytoplankton Associated With Wind Speed and Direction in the Marian Cove, Antarctica. *Front. Mar. Sci.* 9, 887909. <https://doi.org/10.3389/fmars.2022.887909>
- Kranz, S.A., Levitan, O., Richter, K.-U., Prášil, O., Berman-Frank, I., Rost, B., 2010. Combined Effects of  $\text{CO}_2$  and Light on the  $\text{N}_2$  -Fixing Cyanobacterium *Trichodesmium* IMS101: Physiological Responses. *Plant Physiol.* 154, 334–345. <https://doi.org/10.1104/pp.110.159145>
- 520 Lacarra, M., Houssais, M.-N., Sultan, E., Rintoul, S.R., Herbaut, C., 2011. Summer hydrography on the shelf off Terre Adélie/George V Land based on the ALBION and CEAMARC observations during the IPY. *Polar Science* 5, 88–103. <https://doi.org/10.1016/j.polar.2011.04.008>
- Leventer, A., Domack, E., Dunbar, R., Pike, J., Stickley, C., Maddison, E., Brachfeld, S., Manley, P., McClenen, C., 2006. Marine sediment record from the East Antarctic margin reveals dynamics of ice sheet recession. *Gsa Today* 16, 4.
- 525 <https://doi.org/10.1130/GSAT01612A.1>
- Louda, J.W., Li, J., Liu, L., Winfree, M.N., Baker, E.W., 1998. Chlorophyll-*a* degradation during cellular senescence and death. *Organic Geochemistry* 29, 1233–1251. [https://doi.org/10.1016/S0146-6380\(98\)00186-7](https://doi.org/10.1016/S0146-6380(98)00186-7)
- Lourey, M.J., Trull, T.W., Sigman, D.M., 2003. Sensitivity of  $\delta^{15}\text{N}$  of nitrate, surface suspended and deep sinking particulate nitrogen to seasonal nitrate depletion in the Southern Ocean. *Global Biogeochemical Cycles* 17, 2002GB001973.
- 530 <https://doi.org/10.1029/2002GB001973>
- Marcks, B.A., Dos Santos, T.P., Lessa, D.V.O., Cartagena-Sierra, A., Berke, M.A., Starr, A., Hall, I.R., Kelly, R.P., Robinson, R.S., 2023. Glacial Southern Ocean Expansion Recorded in Foraminifera-Bound Nitrogen Isotopes From the Agulhas Plateau



- During the Mid-Pleistocene Transition. *Paleoceanog and Paleoclimatol* 38, e2022PA004482.  
<https://doi.org/10.1029/2022PA004482>
- 535 Massé, G., Belt, S.T., Crosta, X., Schmidt, S., Snape, I., Thomas, D.N., Rowland, S.J., 2011. Highly branched isoprenoids as proxies for variable sea ice conditions in the Southern Ocean. *Antarctic science* 23, 487–498.  
<https://doi.org/10.1017/S0954102011000381>
- Matsuoka, K., Skoglund, A., Roth, G., De Pomereu, J., Griffiths, H., Headland, R., Herried, B., Katsumata, K., Le Brocq, A., Licht, K., Morgan, F., Neff, P.D., Ritz, C., Scheinert, M., Tamura, T., Van De Putte, A., Van Den Broeke, M., Von  
540 Deschwanden, A., Deschamps-Berger, C., Van Liefferinge, B., Tronstad, S., Melvær, Y., 2021. Quantarctica, an integrated mapping environment for Antarctica, the Southern Ocean, and sub-Antarctic islands. *Environmental Modelling & Software* 140, 105015. <https://doi.org/10.1016/j.envsoft.2021.105015>
- McMullen, K., Domack, E., Leventer, A., Olson, C., Dunbar, R., Brachfeld, S., n.d. Glacial morphology and sediment formation in the Mertz Trough, East Antarctica.
- 545 Naeher, S., Suga, H., Ogawa, N.O., Schubert, C.J., Grice, K., Ohkouchi, N., 2016. Compound-specific carbon and nitrogen isotopic compositions of chlorophyll a and its derivatives reveal the eutrophication history of Lake Zurich (Switzerland). *Chemical Geology* 443, 210–219. <https://doi.org/10.1016/j.chemgeo.2016.09.005>
- Needoba, J.A., Sigman, D.M., Harrison, P.J., 2004. THE MECHANISM OF ISOTOPE FRACTIONATION DURING ALGAL NITRATE ASSIMILATION AS ILLUMINATED BY THE<sup>15</sup> N/<sup>14</sup> N OF INTRACELLULAR NITRATE<sup>1</sup>. *Journal*  
550 *of Phycology* 40, 517–522. <https://doi.org/10.1111/j.1529-8817.2004.03172.x>
- Ogawa, N.O., Nagata, T., Kitazato, H., and Ohkouchi, N. (2010) Ultra-sensitive elemental analyzer/isotope ratio mass spectrometer for stable nitrogen and carbon isotope analyses. *Earth, Life, and Isotopes* (Eds. Ohkouchi N, Tayasu I, Koba K), Kyoto University Press, pp.339-353. Ohkouchi, N., Kashiyama, Y., Kuroda, J., Ogawa, N.O., Kitazato, H., 2006. The importance of diazotrophic cyanobacteria as primary producers during Cretaceous Oceanic Anoxic Event 2. *Biogeosciences*  
555 3, 467–478. <https://doi.org/10.5194/bg-3-467-2006>
- Ohkouchi, N., Nakajima, Y., Okada, H., Ogawa, N.O., Suga, H., Oguri, K., Kitazato, H., 2005. Biogeochemical processes in the saline meromictic Lake Kaiike, Japan: implications from molecular isotopic evidences of photosynthetic pigments. *Environmental Microbiology* 7, 1009–1016. <https://doi.org/10.1111/j.1462-2920.2005.00772.x>
- Ohkouchi, N., Takano, Y., 2014. Organic Nitrogen: Sources, Fates, and Chemistry, in: *Treatise on Geochemistry*. Elsevier,  
560 pp. 251–289. <https://doi.org/10.1016/B978-0-08-095975-7.01015-9>
- Otero, X.L., De La Peña-Lastra, S., Pérez-Alberti, A., Ferreira, T.O., Huerta-Diaz, M.A., 2018. Seabird colonies as important global drivers in the nitrogen and phosphorus cycles. *Nat Commun* 9, 246. <https://doi.org/10.1038/s41467-017-02446-8>
- Parish, T.R., Wendler, G., 1991. The katabatic wind regime at Adelie Land, Antarctica. *Intl Journal of Climatology* 11, 97–107. <https://doi.org/10.1002/joc.3370110108>
- 565 Petty, A.A., Holland, P.R., Feltham, D.L., 2014. Sea ice and the ocean mixed layer over the Antarctic shelf seas. *The Cryosphere* 8, 761–783. <https://doi.org/10.5194/tc-8-761-2014>



- Pierella Karlusich, J.J., Pelletier, E., Lombard, F., Carsique, M., Dvorak, E., Colin, S., Picheral, M., Cornejo-Castillo, F.M., Acinas, S.G., Pepperkok, R., Karsenti, E., De Vargas, C., Wincker, P., Bowler, C., Foster, R.A., 2021. Global distribution patterns of marine nitrogen-fixers by imaging and molecular methods. *Nat Commun* 12, 4160. <https://doi.org/10.1038/s41467-021-24299-y>
- 570 Raes, E.J., Van De Kamp, J., Bodrossy, L., Fong, A.A., Riekenberg, J., Holmes, B.H., Erler, D.V., Eyre, B.D., Weil, S.-S., Waite, A.M., 2020. N<sub>2</sub> Fixation and New Insights Into Nitrification From the Ice-Edge to the Equator in the South Pacific Ocean. *Front. Mar. Sci.* 7, 389. <https://doi.org/10.3389/fmars.2020.00389>
- Rafter, P.A., Sigman, D.M., 2016. Spatial distribution and temporal variation of nitrate nitrogen and oxygen isotopes in the upper equatorial Pacific Ocean: Equatorial Pacific nitrate N and O isotopes. *Limnol. Oceanogr.* 61, 14–31. <https://doi.org/10.1002/lno.10152>
- 575 Ratnarajah, L., Puigcorbé, V., Moreau, S., Roca-Martí, M., Janssens, J., Corkill, M., Duprat, L., Genovese, C., Lieser, J., Masqué, P., Lannuzel, D., 2022. Distribution and export of particulate organic carbon in East Antarctic coastal polynyas. *Deep Sea Research Part I: Oceanographic Research Papers* 190, 103899. <https://doi.org/10.1016/j.dsr.2022.103899>
- 580 Riaux-Gobin, C., Poulin, M., Dieckmann, G., Labrune, C., Vétion, G., 2011. Spring phytoplankton onset after the ice break-up and sea-ice signature (Adélie Land, East Antarctic. *Polar Research*.
- Rintoul, S.R., Naveira Garabato, A.C., 2013. Dynamics of the Southern Ocean Circulation, in: *International Geophysics*. Elsevier, pp. 471–492. <https://doi.org/10.1016/B978-0-12-391851-2.00018-0>
- Robinson, R.S., Brunelle, B.G., Sigman, D.M., 2004. Revisiting nutrient utilization in the glacial Antarctic: Evidence from a new method for diatom-bound N isotopic analysis. *Paleoceanography* 19, 2003PA000996. <https://doi.org/10.1029/2003PA000996>
- 585 Robinson, R.S., Kienast, M., Luiza Albuquerque, A., Altabet, M., Contreras, S., De Pol Holz, R., Dubois, N., Francois, R., Galbraith, E., Hsu, T., Ivanochko, T., Jaccard, S., Kao, S., Kiefer, T., Kienast, S., Lehmann, M., Martinez, P., McCarthy, M., Möbius, J., Pedersen, T., Quan, T.M., Ryabenko, E., Schmittner, A., Schneider, R., Schneider-Mor, A., Shigemitsu, M., Sinclair, D., Somes, C., Studer, A., Thunell, R., Yang, J., 2012. A review of nitrogen isotopic alteration in marine sediments. *Paleoceanography* 27, 2012PA002321. <https://doi.org/10.1029/2012PA002321>
- Robinson, R.S., Meyers, P.A., 2002. Biogeochemical changes within the Benguela Current upwelling system during the Matuyama Diatom Maximum: Nitrogen isotope evidence from Ocean Drilling Program Sites 1082 and 1084. *Paleoceanography* 17. <https://doi.org/10.1029/2001PA000659>
- 590 Sachs, J.P., Repeta, D.J., Goericke, R., 1999. Nitrogen and carbon isotopic ratios of chlorophyll from marine phytoplankton. *Geochimica et Cosmochimica Acta* 63, 1431–1441. [https://doi.org/10.1016/S0016-7037\(99\)00097-6](https://doi.org/10.1016/S0016-7037(99)00097-6)
- Sambrotto, R.N., Matsuda, A., Vaillancourt, R., Brown, M., Langdon, C., Jacobs, S.S., Measures, C., 2003. Summer plankton production and nutrient consumption patterns in the Mertz Glacier Region of East Antarctica. *Deep Sea Research Part II: Topical Studies in Oceanography* 50, 1393–1414. [https://doi.org/10.1016/S0967-0645\(03\)00076-6](https://doi.org/10.1016/S0967-0645(03)00076-6)



- 600 Sedwick, P.N., DiTullio, G.R., 1997. Regulation of algal blooms in Antarctic Shelf Waters by the release of iron from melting sea ice. *Geophysical Research Letters* 24, 2515–2518. <https://doi.org/10.1029/97GL02596>
- Serebrennikova, Y.M., Fanning, K.A., 2004. Nutrients in the Southern Ocean GLOBEC region: variations, water circulation, and cycling. *Deep Sea Research Part II: Topical Studies in Oceanography* 51, 1981–2002. <https://doi.org/10.1016/j.dsr2.2004.07.023>
- 605 Shiozaki, T., Fujiwara, A., Inomura, K., Hirose, Y., Hashihama, F., Harada, N., 2020. Biological nitrogen fixation detected under Antarctic sea ice. *Nat. Geosci.* 13, 729–732. <https://doi.org/10.1038/s41561-020-00651-7>
- Sigman, D.M., Altabet, M.A., McCorkle, D.C., Francois, R., Fischer, G., 1999. The  $\delta^{15}\text{N}$  of nitrate in the southern ocean: Consumption of nitrate in surface waters. *Global Biogeochemical Cycles* 13, 1149–1166. <https://doi.org/10.1029/1999GB900038>
- 610 Smik, L., Belt, S.T., Lieser, J.L., Armand, L.K., Leventer, A., 2016. Distributions of highly branched isoprenoid alkenes and other algal lipids in surface waters from East Antarctica: Further insights for biomarker-based paleo sea-ice reconstruction. *Organic Geochemistry* 95, 71–80. <https://doi.org/10.1016/j.orggeochem.2016.02.011>
- Stirnemann, L., Bornman, T.G., Forrer, H.J., Mirkin, J., Ryan-Keogh, T.J., Flynn, R.F., Dorrington, R.A., Verheye, H.M., Fawcett, S.E., 2024. A Circum-Antarctic Plankton Isoscape: Carbon Export Potential Across the Summertime Southern Ocean. *Global Biogeochemical Cycles* 38, e2023GB007808. <https://doi.org/10.1029/2023GB007808>
- 615 Studer, A.S., Sigman, D.M., Martínez-García, A., Benz, V., Winckler, G., Kuhn, G., Esper, O., Lamy, F., Jaccard, S.L., Wacker, L., Oleynik, S., Gersonde, R., Haug, G.H., 2015. Antarctic Zone nutrient conditions during the last two glacial cycles. *Paleoceanography* 30, 845–862. <https://doi.org/10.1002/2014PA002745>
- Szymczak-Żyła, M., Kowalewska, G., Louda, J.W., 2008. The influence of microorganisms on chlorophyll a degradation in the marine environment. *Limnology & Oceanography* 53, 851–862. <https://doi.org/10.4319/lo.2008.53.2.0851>
- 620 Takahashi, T., Sutherland, S.C., Wanninkhof, R., Sweeney, C., Feely, R.A., Chipman, D.W., Hales, B., Friederich, G., Chavez, F., Sabine, C., Watson, A., Bakker, D.C.E., Schuster, U., Metzl, N., Yoshikawa-Inoue, H., Ishii, M., Midorikawa, T., Nojiri, Y., Körtzinger, A., Steinhoff, T., Hoppema, M., Olafsson, J., Arnarson, T.S., Tilbrook, B., Johannessen, T., Olsen, A., Bellerby, R., Wong, C.S., Delille, B., Bates, N.R., De Baar, H.J.W., 2009. Climatological mean and decadal change in surface ocean pCO<sub>2</sub>, and net sea–air CO<sub>2</sub> flux over the global oceans. *Deep Sea Research Part II: Topical Studies in Oceanography* 56, 554–577. <https://doi.org/10.1016/j.dsr2.2008.12.009>
- 625 Takahashi, T., Sweeney, C., Hales, B., Chipman, D., Newberger, T., Goddard, J., Iannuzzi, R., Sutherland, S., 2012. The Changing Carbon Cycle in the Southern Ocean. *oceanog* 25, 26–37. <https://doi.org/10.5670/oceanog.2012.71>
- Tamsitt, V., Drake, H.F., Morrison, A.K., Talley, L.D., Dufour, C.O., Gray, A.R., Griffies, S.M., Mazloff, M.R., Sarmiento, J.L., Wang, J., Weijer, W., 2017. Spiraling pathways of global deep waters to the surface of the Southern Ocean. *Nat Commun* 8, 172. <https://doi.org/10.1038/s41467-017-00197-0>
- 630



- Tamsitt, V., England, M.H., Rintoul, S.R., Morrison, A.K., 2021. Residence Time and Transformation of Warm Circumpolar Deep Water on the Antarctic Continental Shelf. *Geophysical Research Letters* 48, e2021GL096092. <https://doi.org/10.1029/2021GL096092>
- 635 Tyler, J., Kashiyama, Y., Ohkouchi, N., Ogawa, N., Yokoyama, Y., Chikaraishi, Y., Staff, R.A., Ikehara, M., Bronk Ramsey, C., Bryant, C., Brock, F., Gotanda, K., Haraguchi, T., Yonenobu, H., Nakagawa, T., 2010. Tracking aquatic change using chlorin-specific carbon and nitrogen isotopes: The last glacial-interglacial transition at Lake Suigetsu, Japan. *Geochem Geophys Geosyst* 11, 2010GC003186. <https://doi.org/10.1029/2010GC003186>
- 640 Vaillancourt, R.D., Sambrotto, R.N., Green, S., Matsuda, A., 2003. Phytoplankton biomass and photosynthetic competency in the summertime Mertz Glacier Region of East Antarctica. *Deep Sea Research Part II: Topical Studies in Oceanography* 50, 1415–1440. [https://doi.org/10.1016/S0967-0645\(03\)00077-8](https://doi.org/10.1016/S0967-0645(03)00077-8)
- Venables, H.J., Meredith, M.P., 2014. Feedbacks between ice cover, ocean stratification, and heat content in Ryder Bay, western Antarctic Peninsula. *JGR Oceans* 119, 5323–5336. <https://doi.org/10.1002/2013JC009669>
- 645 Wang, X., Liu, X., Fang, Y., Jin, J., Wu, L., Fu, P., Huang, H., Zhang, H., Emslie, S.D., 2020. Application of  $\delta^{15}\text{N}$  to trace the impact of penguin guano on terrestrial and aquatic nitrogen cycles in Victoria Land, Ross Sea region, Antarctica. *Science of The Total Environment* 709, 134496. <https://doi.org/10.1016/j.scitotenv.2019.134496>
- Wendler, G., Stearns, C., Weidner, G., Dargaud, G., Parish, T., n.d. On the extraordinary katabatic winds of Adélie Land.
- Whitworth, T., Orsi, A.H., Kim, S.-J., Nowlin, W.D., Locarnini, R.A., 2013. Water Masses and Mixing Near the Antarctic Slope Front, in: Jacobs, S.S., Weiss, R.F. (Eds.), *Antarctic Research Series*. American Geophysical Union, Washington, D. C.,
- 650 pp. 1–27. <https://doi.org/10.1029/AR075p0001>
- Williams, G. D., Aoki, S., Jacobs, S.S., Rintoul, S.R., Tamura, T., Bindoff, N.L., 2010. Antarctic Bottom Water from the Adélie and George V Land coast, East Antarctica (140–149°E). *J. Geophys. Res.* 115, 2009JC005812. <https://doi.org/10.1029/2009JC005812>
- 655 Williams, G.D., Nicol, S., Aoki, S., Meijers, A.J.S., Bindoff, N.L., Iijima, Y., Marsland, S.J., Klocker, A., 2010. Surface oceanography of BROKE-West, along the Antarctic margin of the south-west Indian Ocean (30–80°E). *Deep Sea Research Part II: Topical Studies in Oceanography* 57, 738–757. <https://doi.org/10.1016/j.dsr2.2009.04.020>
- Wright, S.W., Van Den Enden, R.L., 2000. Phytoplankton community structure and stocks in the East Antarctic marginal ice zone (BROKE survey, January–March 1996) determined by CHEMTAX analysis of HPLC pigment signatures. *Deep Sea Research Part II: Topical Studies in Oceanography* 47, 2363–2400. [https://doi.org/10.1016/S0967-0645\(00\)00029-1](https://doi.org/10.1016/S0967-0645(00)00029-1)
- 660 Zehr, J.P., Capone, D.G., 2020. Changing perspectives in marine nitrogen fixation. *Science* 368, eaay9514. <https://doi.org/10.1126/science.aay9514>